small NANO MICRO

Microfluidics

Formation of Bubbles in a Multisection Flow-Focusing Junction

*Michinao Hashimoto and George M. Whitesides**

The formation of bubbles in a flow-focusing (FF) junction comprising multiple rectangular sections is described. The simplest junctions comprise two sections (throat and orifice). Systematic investigation of the influence on the formation of bubbles of the flow of liquid and the geometry of the junction identifies regimes that generate monodisperse, bidisperse, and tridisperse trains of bubbles. The mechanisms by which these junctions form monodisperse and bidisperse bubbles are inferred from the shapes of the gas thread during breakup: these mechanisms differ primarily by the process in which the gas thread collapses in the throat and/or orifice. The dynamic self-assembly of bidisperse bubbles leads to unexpected groupings of bubbles during their flow along the outlet channel.

Keywords:
- bubble formation
- dynamic self-assembly
- flow-focusing junctions
- microfluidics
- multiphase flows

1. Introduction

This Full Paper describes the stable formation of trains of mono-, bi-, and tri-disperse bubbles in microfluidic flow-focusing (FF) junctions. The simplest and most extensively studied structure of a FF junction incorporates a narrow, straight junction (the ''orifice''; Figure 1), where a continuous thread of fluid breaks and bubbles or droplets form.[1] We explored the breakup of the gas thread and the formation of bubbles in modified FF geometries in which we replaced the simple orifice with multiple rectangular sections (Figure 1). Each rectangular section acted as a distinct site at which bubbles could form; simple modifications of the geometry of the FF junctions made it possible to generate reproducibly bi- or tridisperse bubbles (e.g., regular patterns of bubbles of two or three distinct sizes) and complex patterns of bubbles. The dynamics of flow that produced these patterns was too complex for us to model quantitatively but we visualized the different patterns of bubbles that formed at each section in the junction and inferred mechanisms of formation of bubbles from these visualizations. The streams of multidisperse bubbles generated in these junctions displayed complex interactions as they flowed downstream in the straight outlet channel; the bubbles eventually formed stable, ordered patterns via dynamic self-assembly through the patterns of flow created by the bubbles.

1.1 Bubbles and Droplets in Microfluidics

Multiphase flows are becoming an important part of applied microfluidics. Bubbles, droplets, and complex emulsions are useful in a range of applications, including syntheses of particles,[2] crystallization of proteins,[3,4] mixing,[5,6] modulation of light,[7] encapsulation of particles and cells,[8,9] and information processing.[10,11] Among many methods to generate emulsions,[12–16] two types of structures for the generation of bubbles and droplets have proved especially useful: one is the ''T-junction'' first described by Thorsen[17] and the other is the FF junction pioneered by Gañán-Calvo et al. for gas bubbles[18] and by Anna et al. for liquid droplets.[1]

The formation of bubbles and droplets takes place via different mechanisms in T-junctions and FF junctions. Both T-junctions[5,17,19,20] and FF junctions[1,3,18,21] have been explored. The FF system demonstrated the greatest flexibility in control over the size, volume fraction, and structure of the emulsions that it generates. One of the most useful characteristics of FF systems is their capability to generate monodisperse particles (polydispersity index, $\sigma < 2\%$).[3]

[*] Dr. M. Hashimoto, Prof. G. M. Whitesides
Department of Chemistry and Chemical Biology
Harvard University
12 Oxford Street, Cambridge, MA 02138 (USA)
E-mail: gwhitesides@gmwgroup.harvard.edu

Supporting Information is available on the WWW under http://www.small-journal.com or from the author.

DOI: 10.1002/smll.200902164

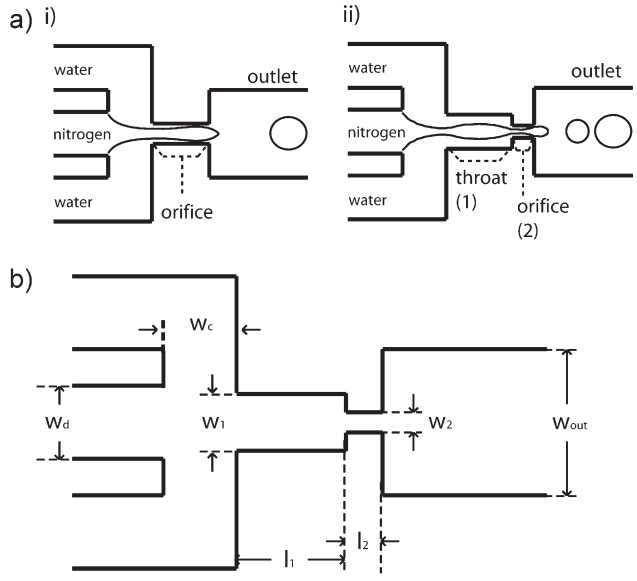

Figure 1. a) Schematic illustration of the flow-focusing junction and definition of the throat and orifice: i) a simple flow-focusing junction; ii) a multiwidth flow-focusing junction. b) Definition of the parameters describing the geometry of the channel. The width and length of the throat are w_1 and l_1, respectively, and the width and the length of the orifice are w_2 and l_2, respectively. Other parameters indicated in the figure are the width of the inlet for the dispersed phase (w_d), the width of the inlets for the continuous phase (w_c), and the width of the outlet channel (w_{out}). In this work, the width of the orifice was always smaller than the width of the throat ($w_1 > w_2$).

Simple modifications of the geometry of the FF junction can add substantial complexity to the processes that generate bubbles. In this work, our aim was to identify the variables – the geometry of the junction and the flows of liquid and gas – that influence the mechanisms that form bubbles. Understanding the formation of emulsions in microfluidic devices has the potential to be useful in applied microfluidics in biology, chemistry,[22] and particle synthesis.[23]

The formation of bubbles and droplets also represents an interesting set of complex nonlinear behaviors. Unexpected behaviors can arise from the processes that form bubbles and droplets, and the interactions between these bubbles and the flowing liquid.[24,25] We believe that microfluidic bubble generators will be useful in studying complexity for three reasons: (i) the mechanism by which a *simple* generator operates is well characterized;[21] (ii) it is easy to fabricate and modify the structure of these generators by soft lithography;[26] (iii) it is possible to use them to create a large number of simple components – bubbles and droplets – and to observe the collective behaviors that emerge from their interactions. The study described here demonstrates the use of microfluidic FF junctions as a testbed with which to explore the unexpected dynamics associated with the formation of bubbles. We rationalized the mechanisms of breakup of the gaseous thread and of the formation of bubbles, based on the well characterized mechanism of formation of monodisperse bubbles, and extended these rationalizations to the generation of bi- and tri-disperse sets of bubbles.

2. Experimental Design

2.1. Geometry of the Orifice and the Dynamics of Breakup of Bubbles

In a FF junction, the processes responsible for the generation of bubbles occur primarily in the junction. Modifications of the geometry of the junction can cause the system to operate in unexpected ways. We have, for example, previously reported stable, long-period oscillatory behavior in the formation of bubbles in multiple FF junctions placed in the channel serially[24] and synchronization of the timing of breakup of threads of gas in multiple FF junctions placed in parallel.[27]

Briefly, a simple FF junction (Figure 1a-i) consists of one inlet in the center for the dispersed phase (here, nitrogen gas), and two inlets that connect perpendicularly to the inlet of the dispersed phase for the continuous phase (here, an aqueous solution of Tween 20, 2 wt%). The three streams of fluid meet in the junction, where the dispersed fluid periodically breaks off in the continuous streams and generates bubbles. The study described here modified the geometry of the previously described FF junctions. In this modified design (Figure 1a-ii), the junction became narrower in steps from upstream to downstream (in contrast to standard FF devices[1,3]). In order to distinguish between them, we call the section with the greater width a *throat*, and the section with the smaller width an *orifice*; correspondingly, we refer to this type of FF junction as a ''two-section FF junction''. The throat section served as another site (in addition to an orifice) where the breakup of a thread of gas could occur.

This small modification to the geometry resulted in unexpected changes in the dynamics of the formation of bubbles. The objective of this research was to investigate (i) the influence of flow (i.e., rate of water and applied pressure of nitrogen gas) on the mechanism of the formation of bubbles, (ii) the influence of the geometries of the multisection junction on the mechanism of breakup of bubbles, and (iii) the dynamic interaction and formation of patterns of bubbles that resulted.

We provide a rationalization for our observations and develop design principles that allow the construction of a device for generating bubbles with a desired combination of sizes.

2.2. Other Parameters Influencing the Performance of FF Nozzles

There are undoubtedly other characteristics (i.e., interfacial tensions, surfactants, wiping, channel dimensions, fluid temperatures, viscosities, etc.) that would make the system behave with different or greater complexity. Our focus in this study was to survey some of the most obvious parameters – the geometry and dimension of the FF nozzle – in one representative system. We chose to explore these parameters, amongst others, because previous studies of the dynamics of breakup of bubbles in a *simple* FF nozzle led us to the hypothesis that the modification of the region would easily change those dynamics. In addition, we anticipated that previous understandings would help rationalize the higher complexity that would arise from such modifications.

Consideration of other parameters, that is, parameters other than the geometries of the nozzle and the flow parameters, would increase the complexity of the system significantly. For example,

we anticipate that the structure and concentrations of surfactants will be important parameters that can influence the complexity of the process that generates bubbles. Figure S1 (see Supporting Information) shows optical micrographs of the outlet channels containing bubbles generated in a simple FF nozzle. In this figure, the flow parameters ($\triangle p$ and Q) were held constant and the concentrations of surfactants were varied. Surfactants in the continuous phase served two purposes: i) preventing the coalescence of generated emulsions by decreasing the interfacial energy between the continuous and dispersed phases and ii) enhancing the wetting of the inner wall of the poly(dimethylsiloxane) (PDMS) channel by the continuous phase by decreasing the interfacial energy between the continuous phase and the solid wall. Both of these considerations were important in achieving stable generation of bubbles. For example, using 0.02% Tween 20, we observed coalescence of bubbles and wetting of the wall by the dispersed phase. We therefore chose to use 2% of Tween 20 to avoid coalescence and wetting.

Another issue was the size of the bubbles. The size depended on the concentration of surfactants (sodium dodecyl sulfate (SDS), 0.01–10%). This observation was most likely explained by the decreased interfacial tension between the water and nitrogen at high concentrations of the surfactant; the interface was easily deformed (eventually leading to pinch off) at low values of this interfacial tension. In other words, the characteristic time required for pinch off (τ_{throat} and τ_{orifice}) became smaller at low values of interfacial tension. These observations indicated that the surfactants, or the interfacial tension, were certainly important parameters determining the pattern of breakup observed in our system.

However, given the complexity of the multiple parameters that influence the system, we limited the focus of this study to an investigation of the geometry of the FF nozzle. We established that variations in geometry of this nozzle *alone* were sufficient to change the pattern of breakup. The work represents an advance in the experimental basis for microfluidics. It would be preferable to develop a generalized theory for this system but, because of the large number of parameters (variables) and the complex behaviors of fluids through the nozzle, we are, so far, limited to retrospective rationalization of experimental observations.

3. Results and Discussion

We first describe the processes that formed groups of gas bubbles with several different discrete sizes in a two-section FF junction. Preliminary observations suggested that (i) the rates of flow of fluids in the system and (ii) the geometry and physical dimensions of the FF junction determined, or influenced, the mechanism of breakup of the bubbles. We surveyed the effects of those parameters on the mechanism of formation of bubbles and on the dispersity and patterns of bubbles.

3.1. Variation in Parameters of Flow

In this section, we describe the mechanism of formation of bubbles in two-section junctions in response to changes in the rate of flow of water and the applied pressure of nitrogen. Two flow parameters governed the generation of bubbles in the FF system: Δp, the pressure drop of nitrogen gas across the FF system (i.e., the dispersed phase that formed bubbles), and Q, the rate of flow of water (i.e., the continuous phase that served as a bulk medium surrounding the bubbles). A previous study of the formation of monodisperse bubbles in a simple FF geometry showed that the volume of individual bubbles (V_b) scales as $V_b \propto \Delta p/\mu Q$.[3,21] The collapse of the neck occurred in the narrow region where three streams met; the scaling suggested that the volume of the bubbles was proportional to the speed of the advance of the thread of gas (Δp) and the time required for the thread of gas to collapse (Q^{-1}) for a fixed viscosity of the continuous phase (μ). We did not vary the viscosity of the continuous phase in this study.

This same scaling was, however, not generally applicable in two-section junctions. The collapse of the thread of gas could take place in either a throat or an orifice and the interplay of the timing of the collapse of the thread of gas, and the advance of the thread of gas, led to different bubble-breakup mechanisms. As a result, the system generated bubbles with different sizes. We observed five patterns of breakup in response to the variation of Δp and Q. We name these five regimes *polydisperse*, *monodisperse(1)*, *bidisperse(1–2)*, *bidisperse(2–1)*, and *monodisperse(2)*. (The following section outlines our observations summarizing the pattern of formation of bubbles in each of these five regimes.) The nomenclature *(1)* denotes collapse of the gas thread or bubble in the *first* section (i.e., throat) and the notation *(2)* denotes the collapse of the gas thread or bubble in the *second* section (i.e., orifice) in the two-section junction; the hyphenated numbers denote the positions and order of the breakup. For example, the notation *bidisperse(2–1)* indicates that the system generated a bidisperse set of bubbles as the result of breakup beginning in the *second* section (i.e., orifice, or *2*) and subsequently in the *first* section (i.e., throat, or *1*).

3.1.1. Polydisperse

In this regime, the system generated polydisperse bubbles (Figure 2b-iv). We observed this regime at a low rate of flow ($Q \approx 0.25$ mL h^{-1}) across a wide range of applied pressure of nitrogen (p). The position of the pinch off of the thread of gas seemed to be random; we observed that the gas thread retracted entirely out of the FF junction, and also remained in the throat and produced bursts of bubbles. This behavior resulted from a relatively low rate of flow of continuous phase and dispersed phase. For each measurement, we waited three minutes after changing the flow parameters. The system did not exhibit any periodic behavior, unlike the other regimes described below.

3.1.2. Monodisperse(2)

In this regime, the breakup of the thread of gas took place only in the orifice during each cycle of the formation of bubbles. The thread of nitrogen gas remained elongated to the orifice and always collapsed in the orifice (Figure 2b-v: $t = 1$ ms). During each cycle, after each pinch off, the thread of gas retracted slightly but remained elongated across the throat, and broke up again in the orifice. A low rate of flow of continuous phase allowed the thread to extend through the throat without collapse. This cycle led to the formation of monodisperse

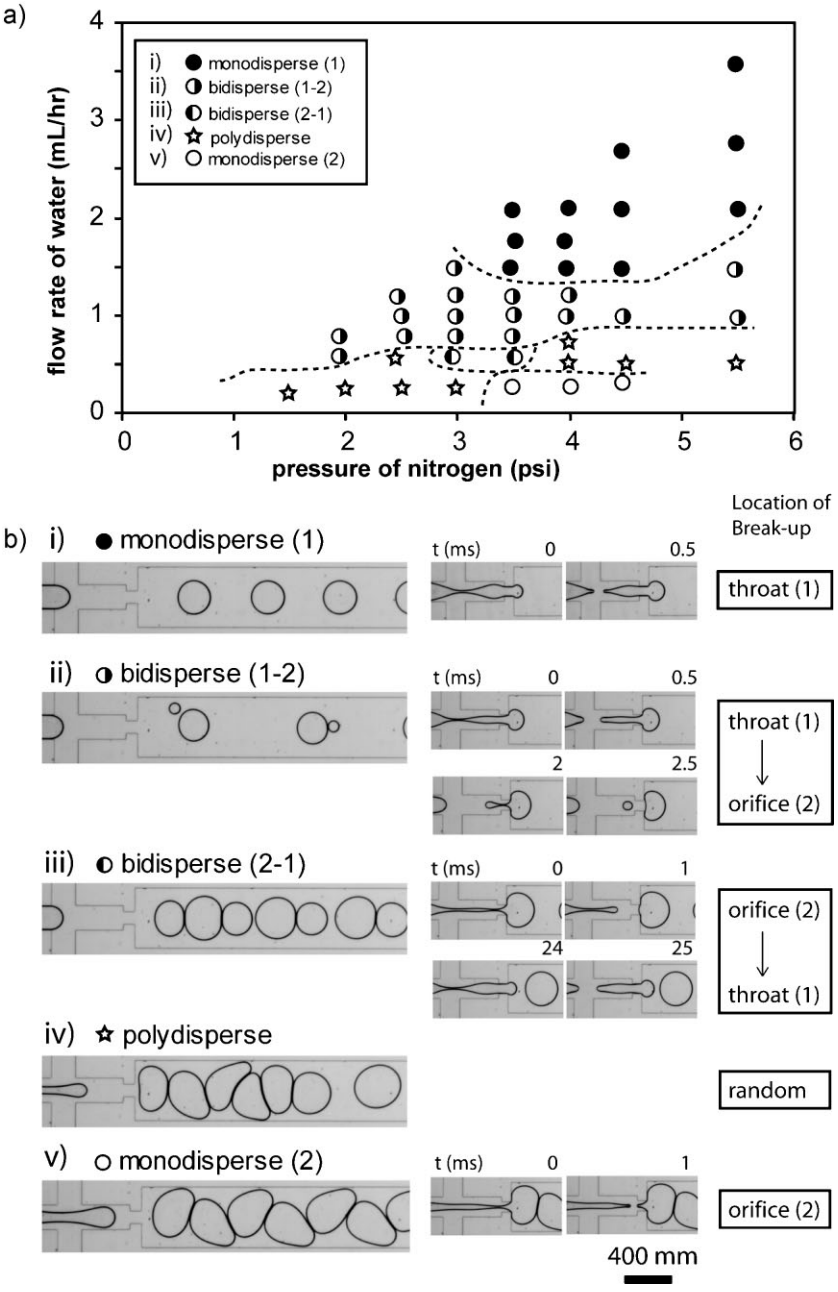

Figure 2. a) A phase diagram summarizing the mechanism of formation of bubbles as a function of the pressure of nitrogen (dispersed phase) and the rate of flow of water (continuous phase). The vertical axis represents Q, the rate of flow of water (continuous phase) and the horizontal axis represents Δp, the applied pressure of nitrogen (dispersed phase). The dimensions of the junction (in mm) were $w_1 = 200$, $l_1 = 400$, $w_2 = 100$, and $l_2 = 100$, respectively. b) Representative images of the five regimes of breakup indicated by the legend.

bubbles. We observed this type of breakup at relatively low rates of flow ($Q \approx 0.25\,\text{mL h}^{-1}$) and high pressures of gas ($p \approx 3.5$–4.5 psi).

3.1.3. Bidisperse(2–1)

At intermediate rates of flow ($Q \approx 1.0\,\text{mL h}^{-1}$), the system generated bidisperse sets of bubbles across a wide range of applied pressures of gas ($p \approx 2.5$–5.5 psi). Each cycle involved two distinct breakup events and generated two bubbles with different sizes. At relatively low rates of flow, the thread of gas broke up in the orifice first (Figure 2b-iii: $t = 1$ ms); after the first breakup, the second breakup occurred in the throat (Figure 2b-iii: $t = 25$ ms).

3.1.4. Bidisperse(1–2)

Upon increasing the rate of flow of continuous phase, the system exhibited a different mechanism for the formation of a bidisperse set of bubbles. In this mechanism, the first breakup occurred in the throat to form a bubble. We referred to the bubble formed in this cycle as a mother bubble (Figure 2b-ii: $t = 0.5$ ms). The mother bubble broke up again into two bubbles while traveling in the orifice (Figure 2b-ii: $t = 2.5$ ms). While the mother bubble traveled through the orifice, a large volume fraction of the bubble remained in the throat; the mother bubble itself blocked the orifice and the stream of the continuous phase caused the second breakup by pinching off the tail of the mother bubble. We referred to the two bubbles formed in this cycle as daughter bubbles.

3.1.5. Monodisperse(1)

At an even higher rate of flow of continuous phase ($Q > 2.0\,\text{mL h}^{-1}$), the system generated monodisperse bubbles (Figure 2b-i). The breakup of the thread took place exclusively in the throat. The bubble generated in the throat passed through the orifice to the outlet channel without further breakup events.

In summary, the thread of gas could collapse either in the throat or the orifice, depending on the flow parameters. The locations of the breakup of the gas thread, and the resulting sizes of bubbles led to the formation of different patterns of monodisperse, bidisperse, or polydisperse bubbles.

3.2. Transition Between Different Mechanisms of Breakup

Variation in the flow parameters induced different patterns of formation of bubbles by changing the positions of the thread of gas at which pinch off took place. Our study suggested that initial breakup took place in the throat (i.e., the first section) at relatively high rates of flow and in the orifice (i.e., the second section) at relatively low rates of flow. The observation could be rationalized by considering the relative significance of three timescales: i) the time required for the collapse of the thread in the throat (τ_{throat}); ii) the time required for the collapse of the thread in the orifice (τ_{orifice});

NANO MICRO small

iii) the time required for the thread to advance from the throat to the orifice ($\tau_{advance}$).

The initial breakup took place in the throat when Equation 1a, or equivalently 1b, described the system:

$$\tau_{throat} < \tau_{advance} + \tau_{orifice} \quad (1a)$$

$$\tau_{throat} - \tau_{orifice} < \tau_{advance} \quad (1b)$$

On the other hand, the initial breakup took place in the orifice when Equation 2a, or equivalently 2b, described the system:

$$\tau_{throat} > \tau_{advance} + \tau_{orifice} \quad (2a)$$

$$\tau_{throat} - \tau_{orifice} > \tau_{advance} \quad (2b)$$

A previous study of the FF generator[21] indicated that the quantity on the left-hand side of Equations 1b and 2b, $\tau_{throat}-\tau_{orifice}$, was a function of the width of the throat and orifice (w_1 and w_2) and of the volumetric flow rate of continuous phase (Q) (i.e., the width of the thread of gas and the rate at which it collapsed.) For a fixed geometry, this quantity decreased with Q (i.e., $\tau_{throat} \propto Q^{-1}$ and $\tau_{orifice} \propto Q^{-1}$) because of the increase in rate of the inflow of continuous phase and, consequently, the increase in the speed of the collapse. The other quantity, $\tau_{advance}$, was the time required for the thread of gas to move through the orifice and was a function of the length of the throat (l_1) and the applied pressure of nitrogen (Δp) (i.e., the speed of the advance of the thread of gas, Q_{gas}, and the distance it traveled); at higher values of Δp, the time required for the thread of gas to advance through a given distance of the throat (l_1) decreased ($\tau_{advance} \propto Q_{gas}^{-1}$ and $Q_{gas} \propto \Delta p$). We therefore anticipated that the initial breakup would occur in the throat at higher values of Q and lower values of Δp. (This expectation agreed with the data described in Figure 2.)

In addition, the decrease in size of the bubbles rationalized the transition from bidisperse(1–2) to monodisperse(1) at higher values of Q. The scaling for the volume of bubbles, $V_b \propto \Delta p/\mu Q$, (with μ fixed in this study) should apply to a simple FF geometry (Figure 1a-i). The generator thus formed smaller bubbles at higher values of Q. Bubbles that were sufficiently small escaped into the outlet channel without experiencing a second breakup and the presence of the orifice did not cause any change in the pattern of the breakup. This process generated monodisperse bubbles.

Examination of the influence of the flow parameters suggested that that the interplay of the timing of the breakup in the throat and the orifice led to different mechanisms. We hypothesized that it would also be possible to control the timing and order of the breakup by changing the *geometry* of the junction.

3.3. Variation in Physical Dimensions of the Junction

We investigated the influence of the dimensions of the junction (i.e., the geometry of the orifice and throat) on the mechanism of generation of bubbles. In the following, we describe and rationalize the breakup patterns observed. We also demonstrate that a more complex geometry of the junction – a junction with three different sections for breakup – could generate tridisperse bubbles reproducibly.

3.3.1. Length of the Throat

We first explored the influence of variations in the length of the throat (l_1) on the performance of the two-section FF junction. The hypothesis was that the length of the throat would alter the position of breakup of the thread of gas by changing the time required for the gas thread to advance through the throat ($\tau_{advance}$, the parameter on the right-hand side of Equations 1b and 2b). Changes in l_1 alone (with p and Q held constant) were sufficient to cause the formation of bubbles to occur by three different mechanisms (bidisperse(1–2), bidisperse(2–1), and monodisperse(2); see Figure 3). For the longest length (400 μm), the breakup was bidisperse(1–2). For intermediate values of l_1 (≈200–300 μm), the breakup pattern was bidisperse(2–1). For small l_1 (=100 μm), the breakup was monodisperse(2).

The relative significance of different time scales (represented by τ_{throat}, $\tau_{orifice}$, and $\tau_{advance}$) rationalized the transition of the mechanism for the breakup. The previous section suggested that the initial breakup took place in the throat if $\tau_{throat}-\tau_{orifice} < \tau_{advance}$ and took place in the orifice if $\tau_{throat}-\tau_{orifice} > \tau_{advance}$ (Equations 1b and 2b). The quantity on the left-hand side of the equation (i.e., $\tau_{throat}-\tau_{orifice}$) was largely constant because we did not change the speed of the continuous phase (and hence the speed of collapse of the gas thread). The parameter on the right-hand side ($\tau_{advance}$, the time required for the thread of gas to advance through the throat) depended on the length of the throat. A longer throat would require more time for the gas thread to travel through it and, therefore, we expected the initial breakup to occur in the throat if the throat was longer.

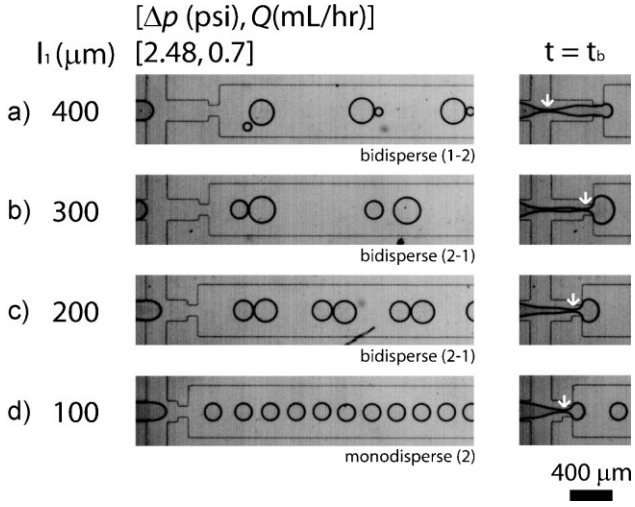

Figure 3. Variation of the length of the throat (l_1) and resulting patterns of bubbles in the outlet channel: a) 400, b) 300, c) 200, and d) 100 μm. The set of images in the right-hand column are instantaneous snapshots of the thread of gas at a time immediately before the first breakup. The breakup occurred in the throat for (a) and in the orifice for (b–d). The white arrows superimposed on the images on the right column indicate the position of the first breakup of each breakup cycle.

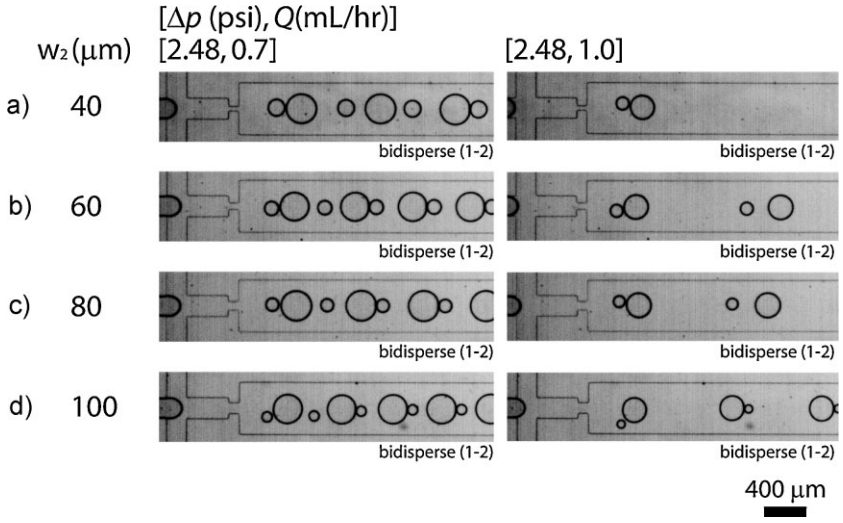

Figure 4. Variations in the width of the orifice (w_2) and resulting patterns of bubbles in the outlet channel: a) 40, b) 60, c) 80, and d) 100 μm.

Our observation supported this hypothesis: the longest throat examined (or, equivalently, the largest $\tau_{advance}$) caused the thread to break in the throat (Figure 3a). When the length of the throat decreased sufficiently, the breakup took place in the orifice (Figure 3d). We considered two asymptotic cases, $l_1 = 0$ and $l_1 = \infty$, to rationalize how the variation of l_1 influenced the mechanism of the breakup for a fixed set of flow parameters. The former would result in the breakup of the thread in the orifice (since the throat would not exist in such a system), while the latter would result in the breakup in the throat (since the length of the throat would be effectively infinite.) We thus anticipated that there existed a critical length of the throat (l_{1*}) for which the location of the *first* breakup switches from the orifice to the throat. The white arrows in the right column of images in Figure 3 indicate the positions of the thread at which initial collapse occurred. For the values of p and Q that we applied in this study, l_{1*} lay between 300 and 400 μm. We note that for an intermediate length of the throat (Figure 3b; $l_1 = 300$ μm), the *second* collapse initiated in the throat during the *first* breakup in the orifice. The emergence of the second point of collapse in the neck, before the completion of the first breakup, allowed less time for the second bubbles to grow and thus generated small second bubbles (Figure 3b). As the length of the throat was made shorter (Figure 3c), the difference in size of the two bubbles also became smaller.

3.3.2. Width of the Orifice

The width of the orifice (w_2) changed the time required for the breakup of the mother bubbles in the orifice and, therefore, the timing of a possible second breakup of a bubble as it passed through the orifice. We observed pronounced changes in the second breakup that formed the daughter bubbles when the system generated bubbles in the bidisperse(1–2) regime.

We varied the width of the orifice and observed the change in the size of the daughter bubbles that formed during the second breakup. Figure 4 shows optical micrographs of arrays of bubbles generated in two-section junctions. The images show a correlation between the widths of the orifice and the size of the rear daughter bubbles (i.e., the smaller bubble in each pair in this example) in the bidisperse(1–2) regime for a fixed set of flow parameters. The rear daughter bubble was larger when the width of the orifice was smaller. Expressed otherwise: the smaller the width of the orifice, the larger the fraction of mother bubbles that remained in the throat during the second breakup in the orifice. (Note that the smaller bubble passed the larger bubble, settled in the front of it, and that the two bubbles flowed together downstream as one assembly; Figure 4d). The details of this process are described in a later section and in Figure 7.

The time required for the collapse of the (mother) bubbles in the orifice ($\tau_{orifice}$) depended on (1) the speed of flow of water that induced collapse in the orifice and (2) the width of the neck of a bubble that collapsed in the orifice. The narrower the orifice, the higher the speed of collapse. For a constant volumetric flow, the local speed of the fluid in the orifice area – and, equivalently, the speed of collapse of the mother bubble – was higher for narrower orifices than for wider orifices. In addition, the width of the orifice was roughly equal to the width of the neck of the bubble that collapsed because the bubble spanned the entire width of the channel when it first entered the orifice. Therefore, the decrease in the width of the orifice caused these two parameters to change in a way that decreased $\tau_{orifice}$ and increased the size of the rear daughter bubbles.

3.3.3. Length of the Orifice

The length of the orifice determined the time required for a bubble to travel through the orifice; the orifice needed to have a minimum length for the mother bubble to collapse and produce two daughter bubbles while it flowed through the orifice. We studied the formation of the daughter bubbles in the orifice (a bidisperse(1–2) regime), and used a sufficiently long throat ($l_1 = 400$ μm) to ensure that the initial breakup occurred in the throat (as described in the previous section that discussed the influence of l_1 on the formation of bubbles.)

Experimental observations supported our hypothesis: for short lengths of the orifice ($l_2 \approx 25$–75 μm; Figure 5a–c), the systems generated arrays of monodisperse bubbles. The pattern was monodisperse(1). For long orifices ($l_2 \approx 100$–150 μm; Figure 5d and e), the second breakup took place in a manner that generated bidisperse(1–2) bubbles. These experiments demonstrated that it was possible to design the channel to generate either monodisperse or bidisperse bubbles simply by changing the length of the orifice.

3.4. Three-Section Junction

We explored whether more complex junction shapes – specifically shapes comprising three sections – would provide additional sites for breakup of bubbles. We tested a FF junction comprising three rectangular sections (which we call a three-section FF junction). We refer to the three sections as first,

NANO MICRO small

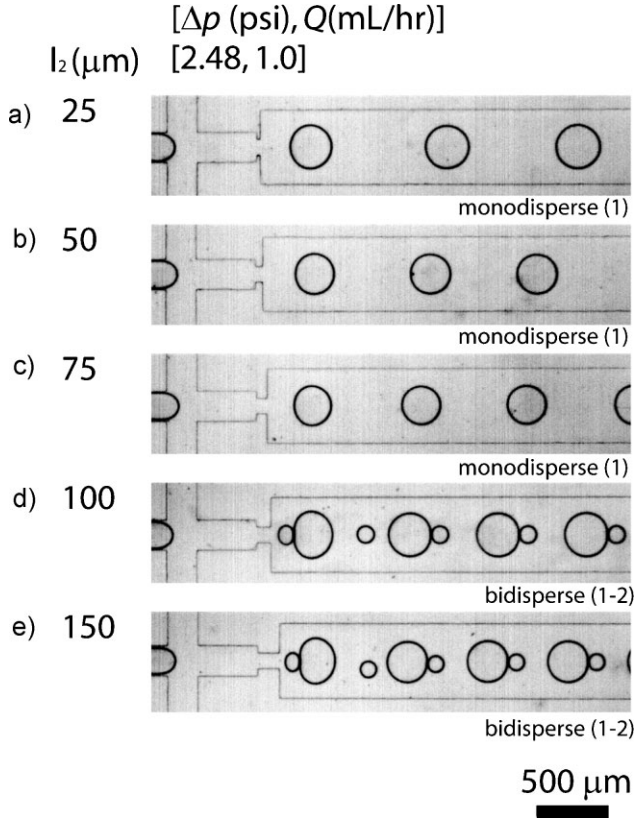

Figure 5. Variation of the length of the orifice (l_2), and resulting patterns of bubbles in the outlet channel: a) 25, b) 50, c) 75, d) 100, and e) 150 μm.

second, and third, moving from upstream to downstream (Figure 6).

The three-section FF junction provided three sites at which a thread of gas could break (Figure 6a and b) and generated a regular sequence of bubbles of three sizes. Figure 6c shows time-resolved images for the progression of the breakup. The breakup pattern was (following the convention used throughout) tridisperse(3–1–2). Complete characterization of this junction would be much more complex than that for the simpler systems; three patterns of monodisperse breakup (i.e., 1, 2, or 3), six patterns of bidisperse breakup (i.e., 1–2, 2–1, 1–3, 3–1, 2–3, or 3–2) and six patterns of tridisperse breakup (1–2–3, 1–3–2, 2–1–3, 2–3–1, 3–1–2, or 3–2–1) would, in principle, be possible (considering all the permutations). In addition, two different events of bidisperse breakup could take place in one cycle (for example, both bidisperse(1–3) and bidisperse(2–3) might take place in one cycle). We have not completely characterized this system but we believe that the design principles inferred from the two-section junction would be generally applicable to the design of systems to generate bubbles with higher dispersity. For example, the observations that (1) an increase in the length of a given section facilitates the formation of bubbles in that section and (2) an increase in the width of a given section increases the time required for the breakup in the section should still hold for a system with a FF junction comprising multiple sections.

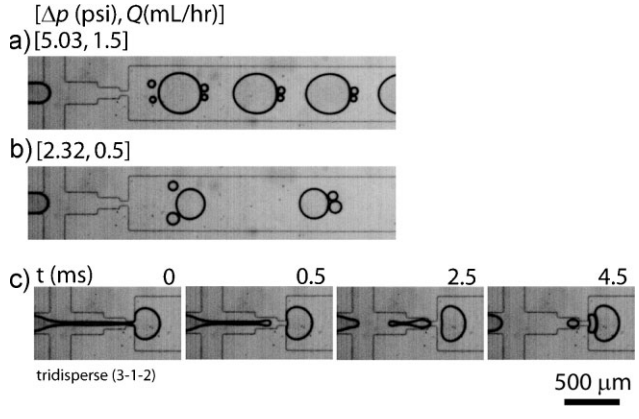

Figure 6. Breakup of the thread of the gas in a three-section junction. a,b) Optical micrographs of tridisperse bubbles formed in the three-width orifice. c) Time-resolved optical micrographs of the thread of gas breaking in the three-width flow-focusing orifice. The numbers on the top-right corner of the images indicate the elapsed time (t) in ms. The time was set to zero in the first image. At $t = 0.5$ ms, the gas thread broke in section 3. The thread slightly retracted and broke in section 1 at $t = 2.5$ ms. Finally, the daughter bubble from the immediately previous breakup went through another breakup at $t = 4.5$ ms in section 2 and thus generated the third bubble.

3.5. Dynamic Pattern Formation in Multidisperse Bubbles

Another interesting phenomenon in these systems was the dynamic self-assembly of patterns of bubbles (Figure 7). Previous studies of the formation of patterns of emulsions include the formation of regular arrays of monodisperse bubbles,[17,18] composite lattices of bubbles and droplets,[28] arrays of nonspherical droplets,[29,30] and fluctuating one-dimensional arrays of bubbles.[25] Here, we observed dynamic self-assembly of multidisperse bubbles into clusters while flowing down the outlet channel. Depending on the size of a large bubble relative to the width of the channel, however, the smaller bubbles took different paths in reaching a stable position with respect to the larger bubble.

Larger bubbles experienced higher flow resistance (i.e., higher drag) than smaller bubbles[31] and thus flowed more slowly in a continuous medium; the largest bubbles traveled at the slowest speed in these systems. In an observation frame that moved at the velocity of flow of the largest bubbles, the continuous phase would be considered as a flow passing periodic circular cylinders (i.e., these large bubbles). It can be seen in Figure 7b and c that smaller bubbles readily deviated from the center of the flow along the extensional flows created by the large bubbles. Over the range of Reynolds numbers under which these experiments were conducted ($Re = \rho v d/\mu \approx 2$, with $\rho = 1\,\mathrm{g\,cm^{-3}}$, $v = 10\,\mu\mathrm{m\ ms^{-1}}$, $d = 200\,\mu\mathrm{m}$, and $\mu = 1\,\mathrm{g\,m^{-1}\,s^{-1}}$), flows past a cylinder started to separate and create recirculating eddies in front of the cylinder.[32] These eddies trapped the smaller bubbles in front of the larger bubbles.

The larger bubbles entered the outlet channel first and the smaller one then followed. We observed two different processes for assembly: i) the smaller bubble was captured by the *next* (following) larger bubble (Figure 7a) and ii) the smaller bubbles passed the side of the larger bubbles, along the extensional

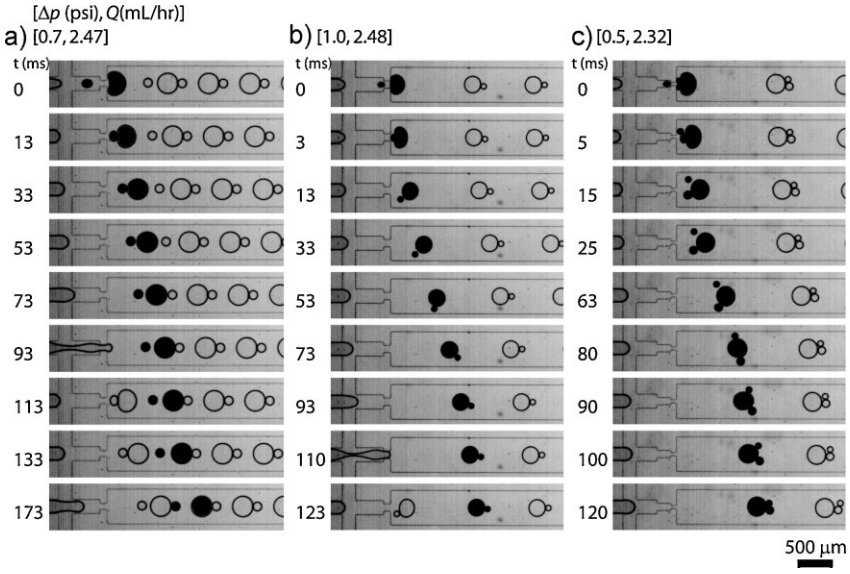

Figure 7. Dynamic self-assembly of bubbles. A single breakup generated one set of bubbles (artificially colored black using Photoshop for easier interpretation). a) Bidisperse bubbles: the larger bubble from one breakup associated with the smaller bubble from the previous break-up. b) Bidisperse bubbles: the large and the small bubbles from a single breakup associated in a process in which the small bubble flowed along the side of the large bubble. c) Tridisperse bubbles: bubbles of three different sizes from a single breakup associated together as the two smaller bubbles flowed around opposite sides of the largest bubble.

fields of flows, and eventually settled in front of the largest bubble (Figure 7b and c). Two or three bubbles associated in a similar way as they flowed in the channel. We believe that three major factors determine the process followed by self-assembly: i) the velocity of the flow of bubbles and continuous phase, ii) the sizes of the small and large bubbles, and iii) the width of the outlet channel. These three variables influenced the fluidic resistance and thus the velocities of the flows associated with the two pathways for assembly (i.e., association of a small bubble with a larger bubble in the front or in the back), and determined the direction of the flow of the small bubbles.

The flow velocities and the sizes of the bubbles were not independent, however, and it was not possible to decouple these two variables in our system. In addition, the fluidic resistance of a given path changed dynamically as the positions of the bubbles and their positions relative to the wall of the channel changed over time. For example, while the small bubble was flowing through a region defined by the large bubble and the wall, the fluidic resistance of the path increased and the velocity of the flow decreased. These characteristics of the system made it difficult to understand the details of the processes involved in the assembly of the bubbles analytically.

4. Conclusions

This Full Paper describes formation of bubbles in a FF junction comprising multiple rectangular sections in the bubble-forming region. We surveyed the flow parameters and the geometries of the FF junction for their influences on the mechanisms that formed bubbles. Our demonstrations suggest that it would be possible to design FF junctions to generate monodisperse, bidisperse, and tridisperse sets of bubbles. The formation of bubbles could, in principle and in practice, occur at any one of the rectangular sections in the junction and the location and order of formation of bubbles determined the size and dispersity of bubbles that the junction generated in each cycle. Our study demonstrates that appropriate designs of the FF junction controlled the dynamics of breakup of the thread of gas and the patterns of bubbles that resulted.

4.1. Study for Complexity and Emergent Behaviors

This work provides examples of complex and emergent behaviors generated by *synthetic* approaches.[21,27] Interactions of the multiple elements (i.e., multiple FF sections and multiple bubbles generated in them) resulted in the complex behaviors observed. FF junctions were fabricated easily using soft lithography and these junctions served as a useful platform for the exploration of complex behaviors in systems that generate bubbles and droplets. In previous work, we observed that relatively simple behaviors suddenly became complex when multiple generators were allowed to interact.[21,27] Many of these complex behaviors could be rationalized retrospectively and qualitatively but not (yet) predicted analytically. Qualitative information, however, may provide useful insights into the overall behavior of the system and allow us to identify the most important interactions. We inferred that the interactions between the processes that form bubbles in each section could be determined by the geometries of these sections. The observations also suggested simple design principles for more complex FF systems comprising multiple sections. We believe that this type of constructionist (in contrast to reductionist) approach (i.e., building complex systems from a well characterized, simple components) should also provide information useful in understanding, and eventually fabricating, complex systems with desired functionalities.

5. Experimental Section

Fabrication of the device: We fabricated the channel system for the microfluidic devices in PDMS slabs using soft lithography and sealed these slabs to a glass cover slide (Corning) using plasma oxidation.[26,33]

Microfluidics: Immediately after sealing the device, we filled the channel of PDMS with an aqueous solution of Tween 20 surfactant (2 wt%; the continuous phase used for the experiment) to ensure that the walls of the microchannels remained

NANO MICRO small

hydrophilic. Nitrogen was the dispersed phase. A digitally controlled syringe pump (Harvard Apparatus, PhD2000 series) delivered the continuous phase to the device at a specified rate of flow. A pressurized tank provided the microfluidic device with gas at constant pressure via a needle valve and a digital manometer (Omega). Polyethylene tubing (PE60, Becton Dickinson) connected the source of the fluid and the PDMS microfluidic channels.

Imaging: A Phantom V9 fast camera and a Nikon objective recorded still images and videos of the image of bubbles. A Leica microscope and the same camera acquired movies and images of the flowing arrays of bubbles.

Acknowledgements

This material is based on work supported by the Department of Energy under award number DE-FG02-00ER45852. We thank Professor Howard Stone for always insightful discussions.

[1] S. L. Anna, N. Bontoux, H. A. Stone, *Appl. Phys. Lett.* **2003**, *82*, 364.
[2] S. Q. Xu, Z. H. Nie, M. Seo, P. Lewis, E. Kumacheva, H. A. Stone, P. Garstecki, D. B. Weibel, I. Gitlin, G. M. Whitesides, *Angew. Chem. Int. Ed.* **2005**, *44*, 724.
[3] P. Garstecki, I. Gitlin, W. DiLuzio, G. M. Whitesides, E. Kumacheva, H. A. Stone, *Appl. Phys. Lett.* **2004**, *85*, 2649.
[4] J-u. Shim, G. Cristobal, D. R. Link, T. Thorsen, Y. Jia, K. Piattelli, S. Fraden, *J. Am. Chem. Soc.* **2007**, *129*, 8825.
[5] J. D. Tice, H. Song, A. D. Lyon, R. F. Ismagilov, *Langmuir* **2003**, *19*, 9127.
[6] P. Garstecki, M. J. Fuerstman, M. A. Fischbach, S. K. Sia, G. M. Whitesides, *Lab Chip* **2006**, *6*, 207.
[7] M. Hashimoto, B. Mayers, P. Garstecki, G. M. Whitesides, *Small* **2006**, *2*, 1292.
[8] S. Takeuchi, P. Garstecki, D. B. Weibel, G. M. Whitesides, *Adv. Mater.* **2005**, *17*, 1067.
[9] A. Huebner, M. Srisa-Art, D. Holt, C. Abell, F. Hollfelder, A. J. deMello, J. B. Edel, *Chem. Commun.* **2007**, 1218.
[10] M. J. Fuerstman, P. Garstecki, G. M. Whitesides, *Science* **2007**, *315*, 828.
[11] M. Prakash, N. Gershenfeld, *Science* **2007**, *315*, 832.
[12] J. M. Gordillo, Z. D. Cheng, A. M. Ganan-Calvo, M. Marquez, D. A. Weitz, *Phys. Fluids* **2004**, *16*, 2828.
[13] Q. Y. Xu, M. Nakajima, *Appl. Phys. Lett.* **2004**, *85*, 3726.
[14] D. R. Link, S. L. Anna, D. A. Weitz, H. A. Stone, *Phys. Rev. Lett.* **2004**, *92*, 054503.
[15] S. Okushima, T. Nisisako, T. Torii, T. Higuchi, *Langmuir* **2004**, *20*, 9905.
[16] A. S. Utada, E. Lorenceau, D. R. Link, P. D. Kaplan, H. A. Stone, D. A. Weitz, *Science* **2005**, *308*, 537.
[17] T. Thorsen, R. W. Roberts, F. H. Arnold, S. R. Quake, *Phys. Rev. Lett.* **2001**, *86*, 4163.
[18] A. M. Gañán-Calvo, J. M. Gordillo, *Phys. Rev. Lett.* **2001**, *87*, 274501.
[19] T. Nisisako, T. Torii, T. Higuchi, *Lab Chip* **2002**, *2*, 24.
[20] P. Garstecki, M. J. Fuerstman, H. A. Stone, G. M. Whitesides, *Lab Chip* **2006**, *6*, 437.
[21] P. Garstecki, H. A. Stone, G. M. Whitesides, *Phys. Rev. Lett.* **2005**, *94*.
[22] H. Song, D. L. Chen, R. F. Ismagilov, *Angew. Chem. Int. Ed.* **2006**, *45*, 7336.
[23] R. K. Shah, H. C. Shum, A. C. Rowat, D. Lee, J. J. Agresti, A. S. Utada, L.-Y. Chu, J.-W. Kim, A. Fernandez-Nieves, C. J. Martinez, D. A. Weitz, *Mater. Today* **2008**, *11*, 18.
[24] P. Garstecki, M. J. Fuerstman, G. M. Whitesides, *Nat. Phys.* **2005**, *1*, 168.
[25] T. Beatus, T. Tlusty, R. Bar-Ziv, *Nat. Phys.* **2006**, *2*, 743.
[26] D. C. Duffy, J. C. McDonald, O. J. A. Schueller, G. M. Whitesides, *Anal. Chem.* **1998**, *70*, 4974.
[27] M. Hashimoto, S. S. Shevkoplyas, B. Zasonska, T. Szymborski, P. Garstecki, G. M. Whitesides, *Small* **2008**, *4*, 1795.
[28] M. Hashimoto, P. Garstecki, G. M. Whitesides, *Small* **2007**, *3*, 1792.
[29] M. Hashimoto, P. Garstecki, H. A. Stone, G. M. Whitesides, *Soft Matter* **2008**, *4*, 1403.
[30] M. Seo, C. Paquet, Z. Nie, S. Xu, E. Kumacheva, *Soft Matter* **2007**, *3*, 986.
[31] H. Wong, C. J. Radke, S. Morris, *J. Fluid Mech.* **1995**, *292*, 95.
[32] M. V. Dyke, *Album of Fluid Motion*, 1st Ed. Parabolic Press, Stanford **1982**.
[33] Y. N. Xia, G. M. Whitesides, *Annu. Rev. Mater. Sci.* **1998**, *28*, 153.

Received: November 16, 2009
Published online: April 21, 2010

